HIGH EFFICIENCY BLUE-GREEN XeF(C -> A) LASER*

Y. Nachshon, F.K. Tittel, and W.L. Wilson, Jr.

Electrical Engineering Department
Rice University
P.O. Box 1892
Houston, TX 77251

and

W.L. Nighan
United Technologies Research Center
East Hartford, CT 06108

Abstract

Blue-green XeF(C) laser output energies in excess of 1 J/l, corresponding to an intrinsic efficiency of ~1.0 per cent have been achieved using e-beam excitation of a unique gas mixture. The relevant parameters which lead to such an efficient broadband blue-green laser are discussed.

Introduction

Recently, significant improvements in the output power and efficiency of the broadband blue-green XeF (C->A) laser have been reported [1],[2]. The output power density of the laser has been increased by almost three orders of magnitude, from less than 0.01 J/l to over 1 J/l, corresponding to an intrinsic electrical-optical energy conversion efficiency of about 1%. These results have been obtained as the result of a much better understanding of the important kinetic and optical absorption issues involved with an electron beam excited XeF (C->A) laser medium, and subsequent tailoring of the laser gas mixture for optimum laser performance.

XeF is unique among the rare gas halides, in that the C(Ω=3/2) excited state is situated nearly 0.1 eV below the B(Ω=1/2) state. Thus, the C state contains more than 95% of the excited state population in thermal equlibrium at room temperature. Because the C state decays to the repulsive A state which lies about ~2.5 eV below it, efficient broadband emission in the blue-green is possible. A number of different workers have reported laser emission from XeF in the blue-green. Pumping methods have included electron-beam excitation [3],[4], direct electrical discharge excitation [5],[6] as well as photolytic pumping of XeF_2 [7],[8]. For all of the electrically excited lasers however, the laser energy and efficiency have been very low.

Kinetic models of the energy deposition and reaction channels leading to formation of excited XeF(C) indicate that the process should be very efficient, and that in spite of the low optical gain resulting from the long lifetime and broad-band nature of the C-A transition, intense blue-green laser emission should result. However, optical probing of the laser gain medium during and after the electron beam pulse showed that significant broadband absorption, resulting from excited and ionized species within the laser medium, was significantly limiting the output power. In this work, carefully planned changes were made to the laser gas mixture. These additions were specifically designed to control or remove the absorbing species and resulted in significant improvements in the XeF (C -> A) laser performance.

Experimental Arrangement

The experimental arrangement used in this work is shown in figure 1. The reaction gases for the XeF (C->A) laser are contained within a stainless steel cell attached to a Physics International Pulserad 110 electron beam machine. A 10 nsec pulse of 1 MeV electrons, with a current density of from 100 to 400 A/cm^2 is injected through a 50 micron titanium foil, which acts as a pressure barrier between the field emission diode of the e-beam machine, and the gas cell. Dielectric mirrors 2.5 cm in diameter, may be mounted inside the cell to form an optical resonator. The temporal behavior of the emission from the cell is monitored with a fast vacuum photodiode connected to a Tektronix 7912 transient digitizer. Color glass and interference filters in front of the diode determine the spectral range of observation. Time-integrated spectral characteristics are obtained with a PAR OMA-1 optical multichannel analyser. Both the OMA and the transient digitizer are connected to a PDP 11/23 minicomputer for data reduction and compilation. Gain characteristics are obtained with an argon ion laser probe beam which passes through the reaction cell and is then monitored with a fast (less than 1 ns rise time) silicon PIN photodiode. An iris in front of the diode, as well as a narrow-band interference filter limit the fluorescence signal which would otherwise currupt the gain data. A mechanical shutter in front of the ion laser limits the probe pulse to 4 msec to avoid saturating the photodiode.

*Work supported in part by the Office of Naval Research, the National Science Foundation and the Welch Foundation.

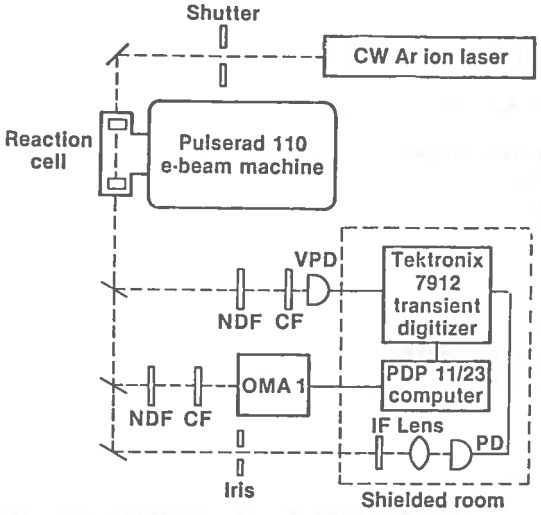

Figure 1. Illustration of the experimental arrangement. NFD: Neutral Density Filter. CF: Color Glass Filter. VPD: Vacuum Photodiode. PD: Silicon PIN Diode.

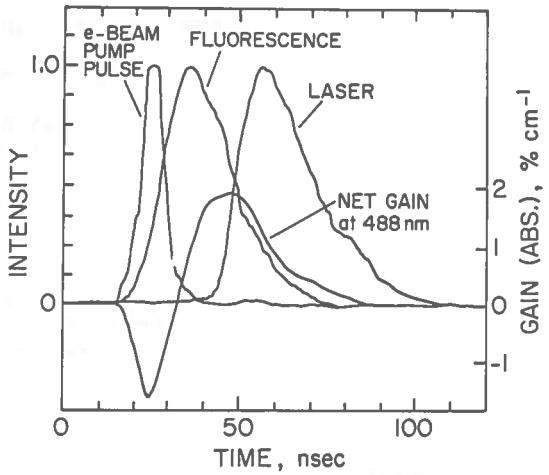

Figure 2. Temporal characteristics of XeF(C->A) Emission. A: e-Beam Current. B: XeF(C->A) Fluorescence. C: Gain/Absorption in the Laser Cavity. D: Laser Emission.

The stainless steel reaction cell was passivated by prolonged exposure to buffered F_2 before any experiments were undertaken. High purity gas mixttures of research grade Ar, Xe, Kr, NF_3 and F_2 were used throughout. Careful monitoring of the exact gas composition for each filling of the cell was done with an MKS Baritron pressure gauge for small percentage constituents, and a precision high pressure gauge for the high pressure buffer gases. A good mix of the constituent gases in the cell was accomplished by turbulent flow of the high pressure buffer gas into the cell during filling. The cell was refilled with a fresh gas mixture after each shot, to avoid depletion and contamination effects.

Experimental Observations

Figure 2 shows the e-beam signal, XeF(C->A) fluorescence, optical gain, and laser emission for a typical gas mixture of 8 torr NF_3, 8 torr F_2, 16 torr Xe, and 6 atm argon. The optical gain was measured using an argon ion laser probe at 488 nm, which is near the peak of the XeF (C->A) fluorescence emission [9]. Curve A represents the e-beam pulse, as measured with a Faraday cup inserted into the cell. Curve B represents the fluorescence from the XeF(C->A) which begins soon after the onset of the e-beam pulse, reaches a maximum when the e-beam curent ceases, and then decays at a rate determined by various quenching processes and the natural lifetime of the excimer. Curve C shows the evolution of the gain/absorption for this gas mixture as a function of time. This curve is typical of the behavior observed for electron beam excited excimer laser media. Beginning with the e-beam pulse there is a rapid build-up of absorption, the result of the creation of various absorbing species in the laser medium. As the XeF(C) state population increases, the net absorption decreases, and finally a net positive gain is observed. Curve D shows that there is a significant delay between the onset of net positive optical gain, and the observation of laser oscillation. This is because with only ~2 % net optical gain, the time required for build-up of the optical flux within the cavity is comparable to the duration of the gain. For this reason, even a modest improvement in the net positive gain can have a very significant effect on laser performance.

Recently, we reported that a two halogen donor mixture of NF_3 and F_2 can lead to in a significant increase in XeF(C->A) laser performance. Although NF_3 has a good electron attachment coefficient for the electron energies encountered in the e-beam environment of our experiments, it is a poor quencher of potential absorbers such as Xe** (6p and 5d). F_2, on the other hand, quenches excited states of Xe quite strongly. Therefore, a combination of the two gases can result in good production of XeF while at the same time, provide a removal channel for Xe**, the primary optical absorber in the after-glow of the e-beam pulse [2]. Although F_2 also quenches XeF(C), it, in combination with the NF_3 in the gas mixture, limits the electron density. Electron quenching of XeF(C) can be significant in e-beam excited mixtures. The net result is an increased XeF(C) population over a moderate range of F_2 concentrations.

Figure 3 shows the effect on the laser output of increasing amounts of F_2 added to a mixture of 8 torr NF_3, 16 torr XE, and 6 atm of Ar. With up to 8 torr of F_2 added to the mixture, the laser output power increases by almost two orders of magnitude. With concentrations of F_2 greater than 8 torr, the effect of F_2 quenching of XeF becomes apparent, and the laser energy falls off. Varying the NF_3 concentration has a much less pronounced effect on the laser output; however, 8 torr represents an optimum value.

Increasing the Ar buffer gas pressure, or increasing the current density injected into the cell (10 atm max and 400 A/cm^2 max) results in increased energy output from the laser. A maximum of 1.0 J/l output energy density, with a 5% output coupler was observed. While concentrations of 8 torr F_2, 8 torr NF_3 and 16 torr Xe are true optimum values, the present levels of current density and the buffer gas pressure represent experimental limitations. Indications are that the laser pulse energy density was increasing somewhat faster than linearly with both of these parameters. Although it is difficult to compute the exact energy deposition into the reaction cell, a careful estimation of the overall conversion efficiency for the XeF(C->A) laser puts the value somewhere between 0.3 and 0.5%, for conversion from the electrical energy deposited in the gas mixture to optical energy coupled out of the cavity.

The effect of the addition of F_2 to the laser gain can be seen in figure 4. Here curve A represents the gain for a 8 torr NF_3 mixture, while curve B represents the gain for a 8 torr NF_3-8 torr F_2 mixture. As is apparent from this figure, the addition of 8 torr F_2 causes a reduction in the initial absorption during the e-beam pulse, and allows the gain to reacher a higher maximum value and to last for a longer period of time. Both of these improvements have a very strong effect on the laser output.

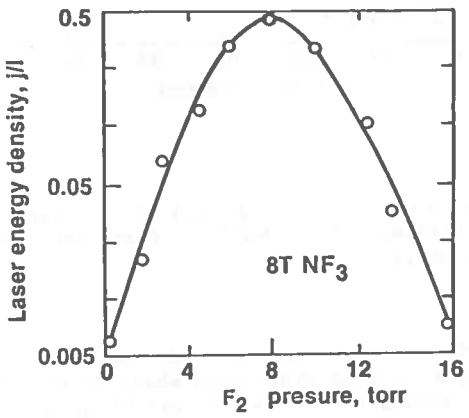

Figure 3. Variation of laser output with F_2 Concentration. Gas mixture laos contains 8 torr NF_3, 16 torr Xe and 6 atm Ar. A 2% output coupler was used in the optical cavity.

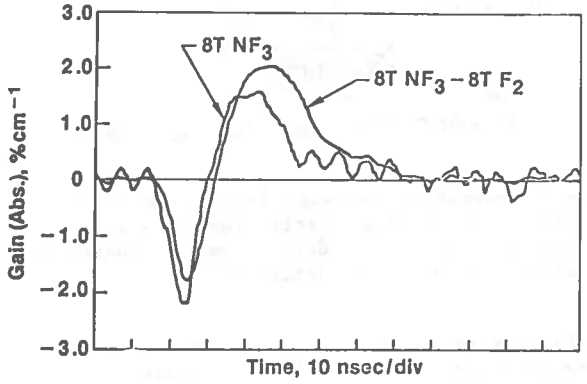

Figure 4. Gain temporal behavior with (A) 8 torr NF_3 and (B) 8 torr NF_3 and 8 torr F_2. Additional gases are 16 torr XE and 6 atm Ar in both cases.

Discussion

In recent years, modeling of the kinetic processes leading to the production and quenching of XeF(B,C) has been the subject of considerable investigation [10],[1]. In this work, the results of these studies, as well as some improvements in rate constants have been used in a self-consistant model for the present experimental conditions. Figure 5 shows the primary pathways leading to the formation and quenching of XeF(B,C). The electron beam energy is deposited in the Argon buffer gas, primary electrons, reacting with neutral Ar result in in excited Ar_2^+. Secondary electrons can also react with Ar to form Ar^+ and Ar_2^{**}. Reaction of these excited argon ion species with xenon result in excited ionic xenon Xe^+ and Xe^{**}. Subsequent ionic recombination with F^- (which was formed by a dissociative attachment reaction between secondary electrons and F_2 or NF_3) results in excited state XeF(B,C). Secondary reactions of Xe with ArF and Ar_2F as well as a reaction between F_2 and Xe^* or Xe^{**} can also result in XeF. The combined production efficiency of the net energy in excited XeF to the total energy deposited in the gas mixture for the present conditions is computed to be about 5-7%. The XeF(B,C) is removed by quenching reactions with Xe, Ar, secondary electrons, and the fluorine donors, as well as by radiative relaxation which gives rise to blue-green photons.

Figure 6 shows the major contributions of the different reactions to the formation of XeF, as well as the relative importance of the various quenching channels which remove XeF. The ionic recombination of F^- with Xe^+ produces almost 50% of the total XeF(B,C) population, while quenching by Xe and F_2 are the two most important removal channels.

Although XeF (B,C) is formed with good efficiency, and the state mixing assured by the large Ar pressure means that almost all of the XeF will be relaxed to the C state, the overall laser efficiency is severely limited by photoabsorption effects. Figure 7 shows the measured optical absorption at 488 nm for a mixture of 6 atm Ar and 16 torr Xe, as well as that for pure argon. The data shown in this figure was repeated for various lines of the Ar+ ion laser, and the results were essentially identical from a wavelength of 457.9 nm to 489 nm [2]. Thus, we conclude that the absorption effects seen here are broad-banded in nature, and extend uniformly across the gain region of interest for XeF(C->A).

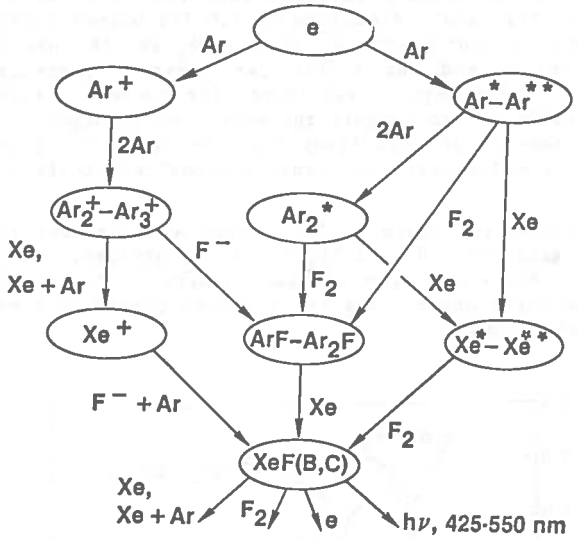

Figure 5. Formation pathways leading to Xef(C) for electron beam excitation of argon, xenon, and F^- donor gas. Quenching mechanisms are also depicted.

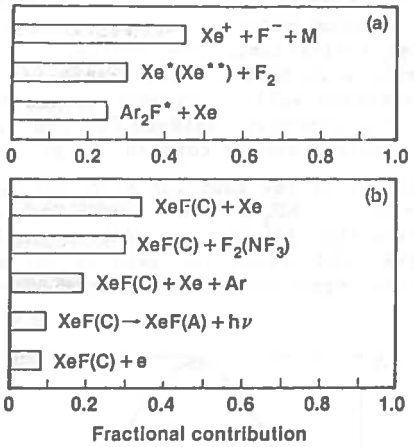

Figure 6. Contributions of each of the various mechanisms to XeF(C) formation and quenching.

With only argon is the cell, a strong absorption (exceeding 9% cm^{-1}) is observed, with two decay rates. One time constant is about 15 nsec, while the second, associated with a less pronounced absorption is about 50 nsec long. Figure 8 (a) shows the calculated excited species concentrations which result from e-beam excitation of Ar. From these results, and published data on the absorption cross section in the blue-green region [12-14] suggest that the strong initial absorption is due to the combined effects of Ar_3^+ and Ar^{**} (4pand3d) while the longer decay-time absorption is due to $Ar_2^*(^3\Sigma_u^+)$ Figure 8 (b) shows the computed fractional contribution of each of these species to the total absorption as a function of time.

When Xe is added to the Ar, the initial absorption is decreased, but a much longer-lived absorption, with a time constant of about 300 nsec appears. The reduction in the initial absorption is the result of charge transfer to the Xe, and are thus rapidly quenched. Of the various Xe products which are produced, analysis shows that only Xe^{**} (6p 5d) have a large enough absorption cross-section to contribute significantly to the blue-green absorption coefficient [2]. Figure 9(a) shows the temporal evolution of the excited species in an Ar-Xe mixture, while Figure 9(b) shows the relative importance of these to the temporal evolution of the absorption.

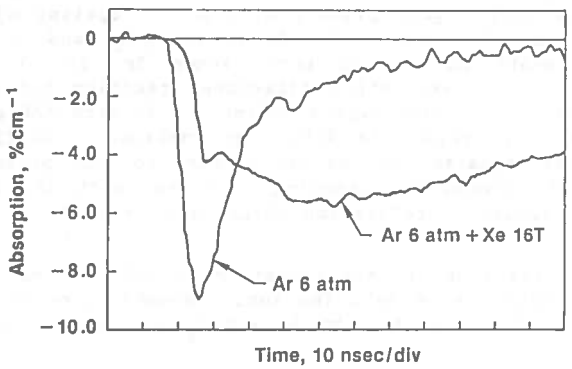

Figure 7. Temporal variation of absorption measured at 488 nm in an e-beam excited gas of 6 atm Ar and in 6 atm Ar with 16 torr Xe.

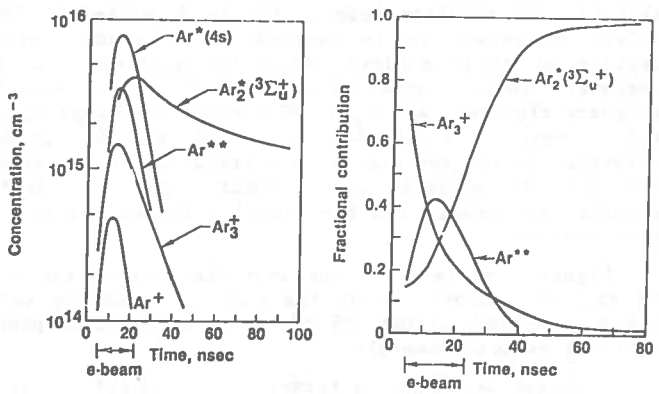

Figure 8. (a) Calculated excited species concentration as a function of time for an e-beam excited gas of 6 atm Ar. (b) Computed fractional contribution of each of the species shown in a) to the absorption at 488 nm.

With the addition of F_2 and NF_3 to the gas mixture of Ar and Xe, the Xe^{**} is also quenched, and so the absorption does not last for as long a time. Most of the quenching of the Xe^{**} comes from reaction with F_2 however. F_2 has the added advantange that it retains a large electron capture cross-section, even down to electron energies as low as 0.1 eV. Thus, with F_2 in the gas mixture, the density of low energy electrons can be significantly reduced. This lowers the electron quenching of XeF(C), and increases the excited state population density, another factor which improves the laser gain. Figure 10 shows the computed absorption as a function of time for a mixture of 8 torr NF_3, 8 torr F_2, 16 torr Xe, and 6 atm Ar, and the contribution from each of the important absorbing species.

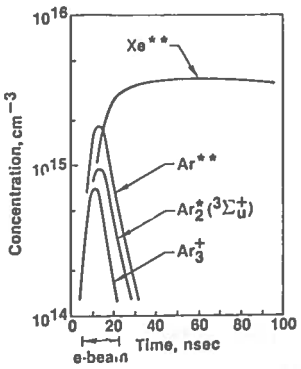

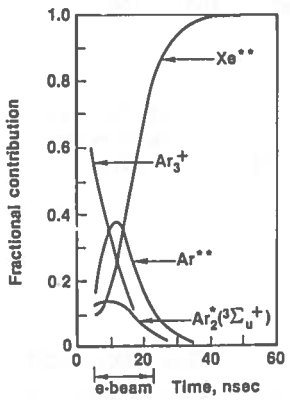

Figure 10. Computed optical absorption at 488 nm as a function of time for an e-beam excited mixture of 8 torr nf3, 8 torr f2, 16 torr Xe and 6 atm Ar.

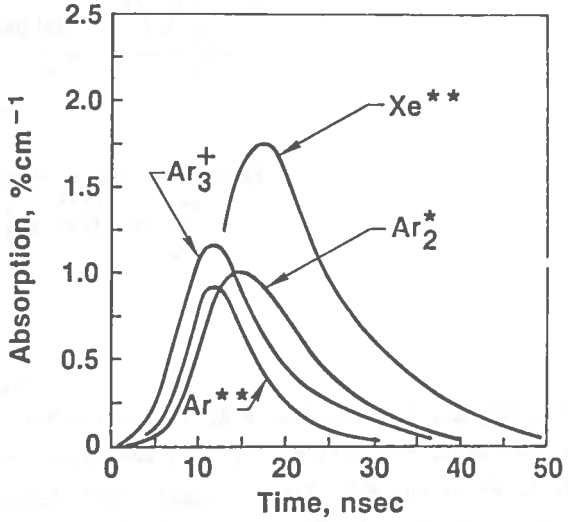

Figure 9. (a) Temporal evolution of important absorbing species in an e-beam excited mixtiure of 16 torr Xe in 6 atm Ar. (b) Computed relative contribution of absorbing species as a function of time.

Figure 11 depicts the computed gain resulting from the XeF(C) state, as obtained from the product of the calculated XeF(C) population density and the stimulated emission cross-section. The net gain, calculated by taking the difference between the XeF(C) gain, and the absorption (figure 10) is also shown. Figure 11 also dépicts the laser intensity build-up in the cavity, calculated from the gain evolution with time. Agreement, both qualitative and quantative with the observed experimental behavior of the e-beam excited XeF(C->A) laser is excellent.

Summary

. In summary, we have shown that the primary factor limiting the performance of the electron-beam excited XeF(C->A) lasers is the presence of broad-band absorbing species created during and after the electron beam pulse. By selection of an appropriate gas mixture - notably one which contains two different fluorine donors, NF_3 and F_2 - we are able to obtain a good formation rate for XeF(C), and at the same time significantly reduce the effect of absorbers. Levels of output power and conversion efficiency have been achieved which make this laser potentially useful for a number of different applications. Computer simulations show that if the initial absorption could be reduced further, and that if the pumping mechanism could provide an active medium for a longer time, much greater improvements in laser performance could be expected.

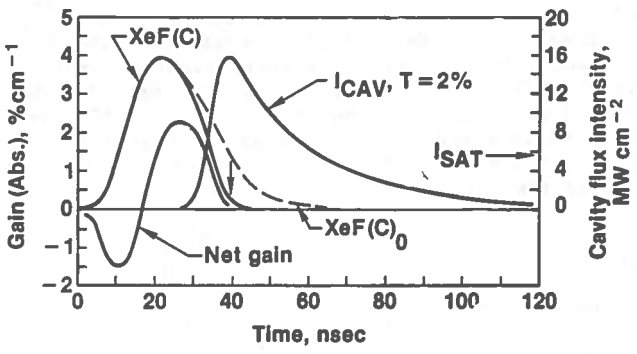

Figure 11. Computed temporal evolution of the net gain, XeF(C) population and intercavity optical flux for the conditions of Figure 10.

References

[1]. W.L. Nighan, Y. Nachshon, F.K. Tittel and W.L. Wilson, Jr., Appl. Phys. Lett., 42, 1006 (1983)

[2]. Y. Nachshon, F.K. Tittel, W.L. Wilson, Jr., and W.L. Nighan submitted to Appl. Phys.

[3]. W. E. Ernst and F.K. Tittel, Appl. Phys. Lett., 35, 36 (1979).

[4]. J.D. Campbell, C.H. Fisher and R.E. Center, Appl. Phys. Lett., 37, 348 (1980).

[5]. R. Burnham, Appl. Phys. Lett., 35, 48 (1979).

[6]. C.H. Fisher, R.E. Cenetr, G.J. Mullaney and J.P. McDaniel, Appl. Phys. Lett., 34, 565 (1979).

[7]. W.K. Bischel, H.H. Nakamo, D.J. Eckstrom, R.M. Hill, D.L. Huestis and D.C. Lorents Appl. Phys. Lett, 34, 565 (1979).

[8] D.J. Eckstrom and H.C. Walker, IEEE J. Quantum Electron., QE-18, 176 (1982).

[9]. G. Marowsky, F.K. Tittel, W.L. Wilson, and E. Frenkel Appl. Opt., 19, 138 (1980).

[10]. J. E. Velazco, J.H. Kolts and D.W. Setser, J. Chem. Phys., 65, 3468 (1976) J. Chem. Phys., 76 4932 (1982).

[12]. C. Duzy and H.A. Hyman Phys. Rev. A22, 1878 (1980).

[13]. H.H. Michels, R.H. Hobbs, and L.A. Wright, Appl. Phys. Lett. 35, 153 (1979)

[13]. W.R. Wadt, Appl. Phys. Lett., 38, 1030 (1981).

[14]. H. H. Michels, private communication.